

# Optimization of C/TiC<sub>x</sub> duplex diffusion barrier coatings for SiC<sub>f</sub>/Ti composites based on interfacial structure evolution exploration

Minjuan Wang<sup>a,b</sup>, Hao Huang<sup>b</sup>, Xu Huang<sup>b\*1</sup>, Mao Wen<sup>c</sup>, Kwang Leong Choy<sup>d\*2</sup>, Cheng Song<sup>a</sup> and Feng Pan<sup>a\*3</sup>

a. Laboratory of Advanced Materials (MOE), School of Materials Science and Engineering, Tsinghua University, Beijing 100084, China

b. AECC Beijing Institute Of Aeronautical Materials, Beijing100095, China

c. College of materials science and engineering, Jilin University, Chang Chun130021, China

d. UCL Institute for Materials Discovery, University College London, London, United Kingdom

## Abstract

Introducing a carbon single coating is a popular method used to protect SiC<sub>f</sub>/Ti composites from severe interface reactions. However, carbon coatings lose their protective effect on SiC fibres at high temperature, even after a short period time. As such, given the strong demand for high temperature applications in aeronautics and astronautics a more coating which is more effective at high temperatures is desirable. In order to improve the high temperature interfacial stability of SiC<sub>f</sub>/Ti composites, a C/TiC<sub>x</sub> duplex coating system with different C contents in TiC<sub>x</sub> was introduced to explore the protection of fibres at 1200°C for 1h. The results show that the C/quasi-stoichiometric TiC coating system protects the SiC fibres most effectively. Based on

---

<sup>1</sup>E-mail: [13910936626@139.com](mailto:13910936626@139.com)

<sup>2</sup>E-mail: [k.choy@ucl.ac.uk](mailto:k.choy@ucl.ac.uk)

<sup>3</sup>E-mail: [panf@mail.tsinghua.edu.cn](mailto:panf@mail.tsinghua.edu.cn)

insights from the evolution of the interface structure,  $TiC_x$  has been identified as an interfacial reaction product from the C single coating, exhibiting a gradient in C content and grain size, which is different from a deposited TiC layer with a well-distributed composition and structure. The different coating structure gives rise to different ability to resist C diffusion at high temperatures, in which poor resistance ability appears in  $TiC_x$  interfacial reaction layer coming from C single coating due to short-circuit diffusion in C-rich fine-grained TiC layer and fast intracrystalline diffusion triggered by amounts of vacancies in sub-stoichiometric coarse-grained TiC layer. Therefore, C/quasi-stoichiometric TiC duplex coatings with a thick, coarse-grained quasi-stoichiometric TiC layer could effectively inhibit C diffusion by comparison to C single coatings, and is more effective than C/rich-carbon TiC duplex coatings due to the existence of short-circuit diffusion in the latter. As such, C/quasi-stoichiometric TiC duplex coatings appear to be an optimal diffusion barrier for  $SiC_f/Ti$  composites at high temperature.

**Keyword:  $SiC_f/Ti$  composites, C single coating, C/ $TiC_x$  duplex coating, quasi stoichiometric ratio of TiC, carbon rich TiC**

## 1. Introduction

Continuous SiC fibre reinforced titanium matrix composites (abbreviated as  $SiC_f/Ti$  composites) have emerged as a promising candidate material for parts of propulsion systems and hypersonic aircraft owing to its significant advantage over conventional materials such as nickel-based superalloy, titanium alloy and steel, with respect to excellent mechanical properties such as high specific strength and modulus at high temperatures [1,2]. Nevertheless, severe interfacial reactions between the titanium alloy and SiC fibres fibre cause degradation of the fibre and, as a result, degrade the mechanical properties of the composites. This is a key limitation for real world applications. For this material system, several strategies have been implemented to inhibit these deleterious interfacial reactions [3]. These include lower temperature consolidation using spark plasma sintering [4,5], the addition of alloying elements to

the Ti matrix [6,7], and coating the fibres with protective layer(s) [8,9]. Among these, coating the fibres with an inert coating system has proved the most viable approach. Until now, carbon coatings have been comprehensively employed as a reaction barrier coating to protect the SiC fibre and minimise interfacial reactions [6,9]. It has been confirmed that carbon coatings, and the TiC interfacial reaction layer perform well during fabrication and in-service at low temperature ( $< 800^{\circ}\text{C}$ ) [10]. However, carbon itself is not a thermo-chemical barrier layer as it reacts with Ti ( $\text{Ti} + \text{C} \rightarrow \text{TiC}$ ,  $950^{\circ}\text{C}$ ,  $\Delta G = -170 \text{ kJ/mol}$  [9]) and hence is rapidly depleted. Thus, interfacial instability occurs at high temperatures (e.g.  $1100^{\circ}\text{C}$ ), even over a relatively short period of time (e.g. 2 hrs) [10]. Therefore, new coating systems are needed for demanding, high temperature applications such as hypersonic flight vehicles. Such applications require a material which can withstand high operating loads while maintaining dimensional stability, mechanical strength and toughness at high-temperatures.

Currently, novel reaction barrier coatings such as chemical vapor deposited (CVD) TiC [3,9],  $\text{TiB}_x$  [9,11,12,13],  $\text{B}_4\text{C}$  [14,15] and Mo [16] are being investigated, along with inner carbon coatings which form C/X (X represents the outer protective coating) duplex coatings at high temperatures. For instance, the inter-diffusion and reaction of Ti/SiC can be effectively inhibited using  $\text{TiB}_2$  protective coatings [9,10], (especially  $0.2 \mu\text{m}$   $\text{TiB}_2$  at the in-service temperature of  $820^{\circ}\text{C}$ ) which shows no apparent interfacial reactions up to  $1000^{\circ}\text{C}$  [9]. However, B-rich  $\text{TiB}_2$  reacts with Ti to form needle/rod-like TiB, which grows rapidly and reduces the effectiveness of the diffusion barrier as the temperature increases further [17,18,19]. Although CVD TiC coatings provide effective diffusion barriers, the high coating deposition temperature leads to a reduction in strength of the SiC fibres. Taking interfacial compatibility into consideration, TiC is the most effective compliant layer for retarding interfacial reactions [3, 9]. Further, it helps to accommodate the thermal residual stress caused by the coefficient of thermal expansion (CTE) mismatch of the carbon coating and titanium alloy matrix [3,9]. Though TiC is also formed by reactions between a carbon coating and titanium alloy, such a reaction results in a steep gradient in composition and microstructure of the resultant TiC layer. In contrast, deliberately prepared TiC coatings can be deposited

with a consistent composition and structure throughout the whole coating. As such there is a significant difference in interfacial stability between C/TiC<sub>x</sub> duplex coating and C single coating systems. However, the interface evolution of the TiC coating/Ti-alloy matrix is poorly understood. Understanding this evolution and the mechanisms by which it occurs would be highly beneficial and provide insights into how to optimise the performance of this system.

This article aims to address this knowledge gap, and enable the optimisation of barrier coating systems for high temperature applications. Based on the literature [20,21], physical vapor deposited (PVD) TiC coatings are widely employed for various applications, however the properties and structure of these coatings are highly depend on C content. Consequently, two TiC coating systems with different C content were designed to optimise interfacial stability at high temperatures in this context. By comparison with the single carbon coating, it has been found that SiC fibres are better preserved under the protection of a C/TiC<sub>x</sub> duplex coating system with a quasi-stoichiometric TiC<sub>x</sub> layer.

## **2. Experimental**

### **2.1 Material preparation**

#### **(a) Protective coating fabrication**

Continuous SiC fibres consisted of a 100 μm diameter SiC monofilament with a 15 μm diameter tungsten core and a 2~3 μm outer layer of a pure carbon protective film (provided by AECC Beijing Institute of Aeronautical Materials, China). In our work, TiC<sub>x</sub> coatings with different compositions were deposited onto the pure carbon coating using a reactive sputtering method based on the reaction of a Ti metal target with methane gas ( $\text{CH}_4^+ + \text{Ti}^- \rightarrow \text{TiC}_x + 2\text{H}_2$ ) to deposit the TiC<sub>x</sub> coating. Deposition was performed in a vacuum of  $1 \times 10^{-4}$  Pa. During the deposition, the temperature of the substrate was maintained at 400 °C, and the flow rates of the Ar carrier gas and CH<sub>4</sub> were precisely controlled to achieve the desired composition. The CH<sub>4</sub> flow rate was controlled at 5 and 30 sccm to react with Ti ions sputtered from Ti target to prepare quasi-stoichiometric TiC<sub>x</sub> (abbreviated as QC-TiC) and carbon rich TiC<sub>x</sub> (abbreviated

as RC-TiC) coatings, respectively. The working pressure was set at 0.8 Pa during all depositions. All obtained TiC coatings were targeted to be 0.8  $\mu\text{m}$  thick.

### **(b) Composite fabrication**

After barrier coatings were fabricated, Ti17 alloy with a nominal composition Ti-5Al-2Sn-2Zr-4Mo-4Cr (wt.%) was deposited on the coated SiC fibres (i.e. C single coating, C/RC-TiC duplex coating and C/QC-TiC duplex coating) using PVD (the wires after PVD deposition defined as precursor wires). Subsequently, the precursor wires were cut to the desired length and encapsulated in the Ti alloy canning using electron beam welding, followed by hot isostatic pressing (HIP) at 920  $^{\circ}\text{C}$  under a gas pressure of 120 MPa for 2 hours to consolidate the SiC<sub>f</sub>/Ti composites. In total, SiC<sub>f</sub>/C/Ti17, SiC<sub>f</sub>/C/RC-TiC/Ti17 and SiC<sub>f</sub>/C/ QC-TiC /Ti17 composites have been fabricated. Subsequently, the rod-like composites were cut into thin sections, with each section then encapsulated in a quartz glass tube and heat treated at 1200  $^{\circ}\text{C}$  for one hour.

## **2.2 Materials testing and characterisation**

The chemical binding state and structure of two kinds of TiC<sub>x</sub> coating were analysed by ESCALAB-250 X-ray photoelectron spectroscopy (XPS), as well as high resolution transmission electron microscopy (HRTEM) of the TiC<sub>x</sub> coating using a field emission JEOL 2010F TEM. The cross-sectional morphologies and chemical composition of the interfacial reaction layers of SiC<sub>f</sub>/C/Ti17 and SiC<sub>f</sub>/C/TiC<sub>x</sub>/Ti17 composites were characterised using a scanning electron microscope (SEM) (FEI nano 450) and Energy dispersive spectroscopy (EDS) (Inca E 350). The microstructures of interfacial reaction layers were observed using a G 20 Ganta Transmission electron microscope (TEM) with a 200 kV electron beam. For TEM specimen preparation, a FEI Quanta 200 FEG Focused Ion Beam (FIB) was used to fabricate thin composite slices with a typical 100~200 nm thickness.

## **3. Results and Discussion**

### **3.1 The interfacial stability of SiC<sub>f</sub>/C/Ti17 composite with C single coating**

The consolidated SiC<sub>f</sub>/C/Ti17 composite was observed to have a 1.8 $\mu\text{m}$  thick interfacial reaction layer after being HIPed at 920 $^{\circ}\text{C}$ /120MPa for 2h, as shown in Fig.

1a. The SiC fibre remained completely intact under the protection of the carbon coating, while a  $\sim 1.4 \mu\text{m}$  thick residual carbon layer survived after the composite fabrication. To assess the high temperature performance of the coating, the  $\text{SiC}_f/\text{C}/\text{Ti17}$  composite was exposed to  $1200^\circ\text{C}$  for 1hr. It was found that serious interfacial reactions occurred between the carbon coating and titanium alloy matrix, totally consuming the carbon coating, which failed to protect the SiC fibre, as evidenced by severe attack from Ti matrix (see Fig. 1d). Moreover, the interfacial reaction results in a significant volume change, causing increased porosity in the vicinity of the interfacial layer, and deformation and fracture of the reaction layer. Consequently, the reinforced SiC fibre reacted with the matrix and was destroyed.

The distributions of C and Ti across the interfacial layer, as calculated using EDS, are shown in Fig. 1b/1c, and 1e/1f, respectively. The C distribution in the as-fabricated composite is clearly confined to a complete region corresponding to the as deposited carbon layer, whereas after heat treatment carbon is consumed seriously and distributed in a highly non-uniform manner which is not indicative of a uniform, adhesive layer. This is consistent with the observation that a single layer carbon coating does not effectively inhibit reactions between the SiC fibre and Ti matrix at high temperatures.

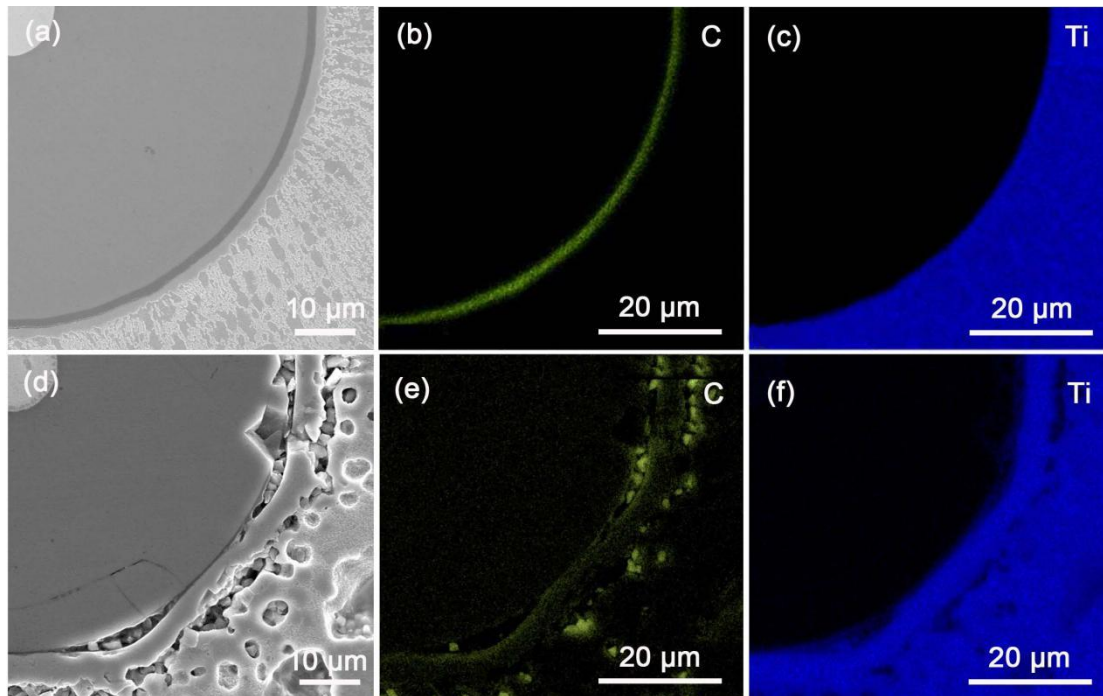


Fig.1 Cross-sectional SEM images of C coated SiC fibre in Ti17 matrix : (a) the

interfacial reaction layer between the fibre and the matrix, (b) carbon elemental mapping; and (c) titanium elemental mapping of the as-fabricated SiC<sub>f</sub>/C/Ti17 composites with C single coating; (d) the interfacial reaction layer between the fibre and the matrix, (e) carbon elemental mapping; and (f) titanium elemental mapping of SiC<sub>f</sub>/C/Ti17 composites with C single coating after 1200 °C for 1 hour.

### 3.2 Interfacial stability of SiC<sub>f</sub>/Ti composites with C/TiC<sub>x</sub> duplex coating

As the single layer carbon coating does not fully protect the SiC fibre from deleterious interfacial reactions at high temperatures, an additional TiC coating was introduced to address this limitation. As a novel compliant layer, two types of TiC<sub>x</sub> coating (RC-TiC and QC-TiC) were deposited onto the carbon coating using reactive magnetron sputtering. XPS was applied to analyse the chemical composition and bonding structure of the TiC<sub>x</sub> coatings, as shown in Fig. 2a and 2b. Both XPS spectra for the two coatings consist of a C-Ti peak centred at ~282.2 eV and a C-C peak at ~284.4 eV, which is only present in the RC-TiC coating [21,22,23]. The C-C peak may arise from both sp<sup>2</sup> and sp<sup>3</sup>-hybridised carbon [24,25], and the C-Ti peak can be associated with a number of Ti-carbide phases. This indicates that only a small amount of C forms crystalline carbide compounds, and that the RC-TiC coating was indeed rich in carbon, with a composition near TiC<sub>1.6</sub>, according to the area ratio between the C-C and C-Ti peaks. Combined with the HRTEM results given in Fig. 2c, amorphous carbon segregates several crystalline particles, identified as cubic TiC, with the diffraction pattern shown in the inset of Fig. 2c. These are globular TiC nanocrystals (marked with white circles in Fig. 2c) with an average size of several nanometers and are covered by a ~10 nm layer of amorphous carbon, which corresponds with the XPS analysis. A large face-centred-cubic (fcc) quasi-stoichiometric grain of TiC is observed in Fig. 2d, with the diffraction pattern shown in the inset figure. This is in agreement with the XPS spectra. Obviously, the TiC crystal grains (~ 20 nm) are noticeably larger than the nanocrystalline (~ 5 nm) TiC grains embedded in the amorphous carbon matrix, which appears to have limited the growth of TiC grains in the RC-TiC coating. The microstructural difference between the two TiC<sub>x</sub> coatings is strongly dependant on the carbon content of the coating, which is also observed in other reported works [20,22].

In addition, a typical SiC fibre with a C/TiC<sub>x</sub> duplex coating (i.e. 2µm /0.8µm) is shown in Fig. 2e to illustrate the coating microstructure.

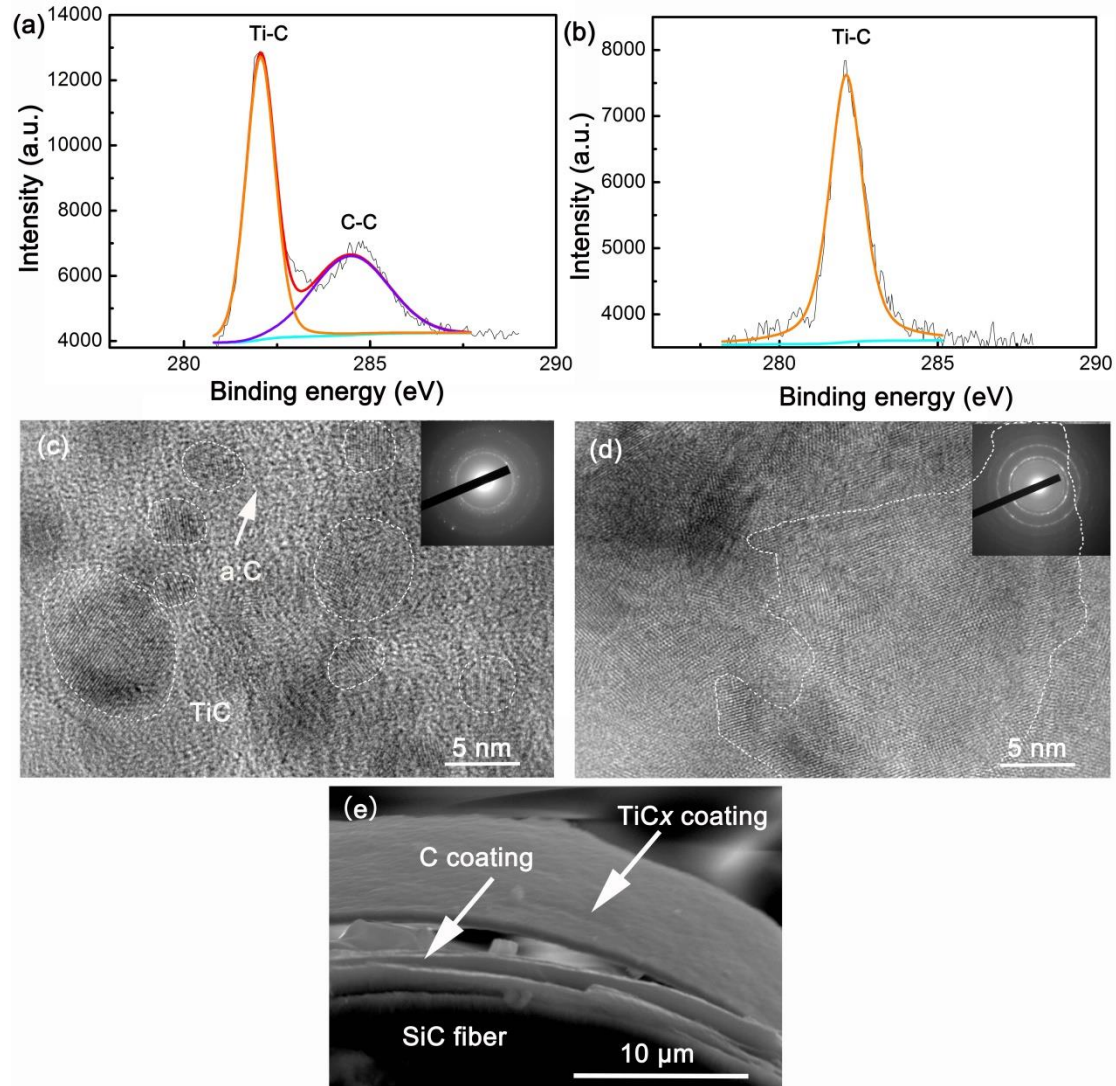


Fig.2 The XPS patterns for (a) RC-TiC coating; and (b) QC-TiC coating; HRTEM images for (c) RC-TiC coating and (d) QC-TiC coating. Inset charts are the diffraction patterns for TiC coatings. (e) The SEM microstructure of the C/TiC<sub>x</sub> duplex coating.

To investigate interfacial chemical stability, identical heat treatments at 1200 °C for 1h were also applied to the SiC<sub>f</sub>/C/TiC<sub>x</sub>/Ti17 composites, and the cross-sectional SEM micrographs obtained. These are exhibited in Fig. 3a-3f. Compared with Fig. 1d, the micrographs presented in fig 3.b and e clearly demonstrate the presence of a non-continuous residual carbon coating, but almost intact SiC fibre in the heat treated SiC<sub>f</sub>/C/TiC<sub>x</sub>/Ti composite, suggesting these coatings may offer superior protection to a C single coating. Upon further examination, a crack is visible around the interfacial



reaction layer in the  $\text{SiC}_f/\text{C}/\text{RC-TiC}/\text{Ti17}$  composite. The reaction layer is  $\sim 6 \mu\text{m}$  thick, and the residual carbon coating is  $\sim 0.6 \mu\text{m}$  thick. The brittle TiC is prone to crack initiation due to the large volume change associated with growth of the interfacial reaction layer. Fortunately, a more favourable, cohesive and adherent interfacial zone is established in the  $\text{SiC}_f/\text{C}/\text{QC-TiC}/\text{Ti17}$  composite, yielding a narrower reaction layer  $\sim 5 \mu\text{m}$  thick and a thicker continuous residual carbon coating layer of  $1 \mu\text{m}$ . This is further confirmed by the compact and continuous distribution of carbon in the layer region in the later composite (fig. 3.e). Taken together, from this evidence it can be concluded that the interfacial stability of the  $\text{SiC}_f/\text{C}/\text{QC-TiC}/\text{Ti17}$  composite is superior to the  $\text{SiC}_f/\text{C}/\text{RC-TiC}/\text{Ti17}$  composite, and much better than  $\text{SiC}_f/\text{C}/\text{Ti17}$  composite. It's noticed that though all of the interfacial reaction zones mainly composed of TiC products in the three composites mentioned above, different phenomenon for interfacial stability observed suggest that the different microstructures of TiC originating from interfacial reactions from the C single coating and, deposited RC-TiC layer and QC-TiC layer, strongly effect the diffusion behaviour.

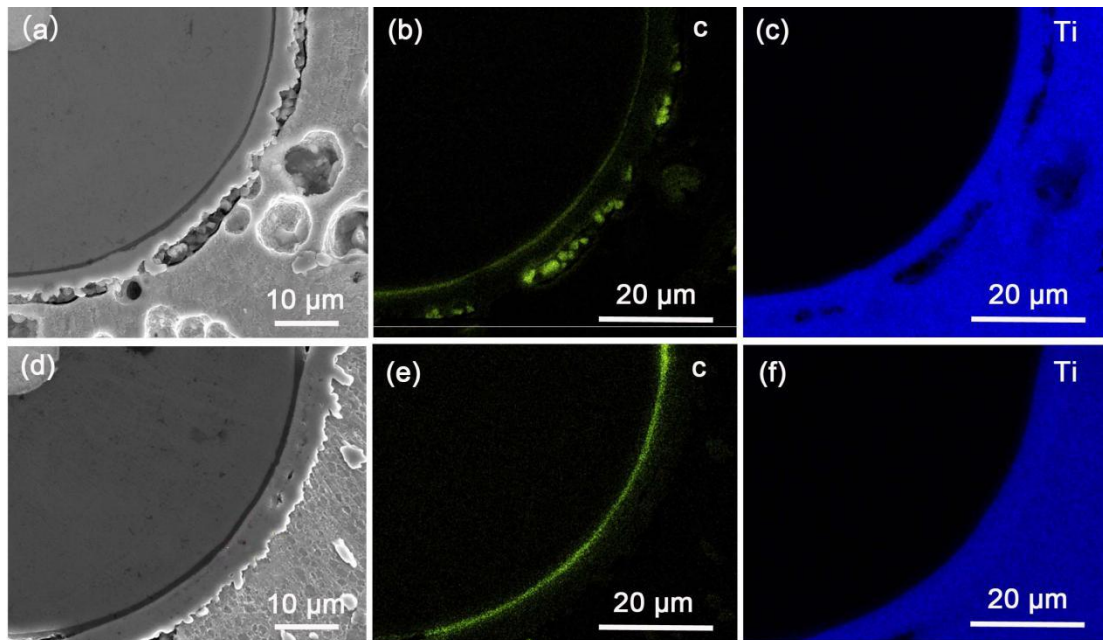


Fig.3 Cross-sectional SEM images of  $\text{C}/\text{TiC}_x$  duplex coating systems in Ti17 matrix : (a) the interfacial reaction layer between the fibre and the matrix, (b) carbon elemental mapping; and (c) titanium elemental mapping of the  $\text{SiC}_f/\text{C}/\text{RC-TiC}/\text{Ti17}$  composites after  $1200 \text{ }^\circ\text{C}/1$  hour heat exposure; (d) the interfacial reaction layer between the fibre

and the matrix, (e) carbon elemental mapping; and (f) titanium elemental mapping of the SiC<sub>f</sub>/C/QC-TiC/Ti17 composites after 1200 °C/1 hour heat exposure.

### 3.3 TEM insights on interfacial evolution

Although the interfacial reaction layer between the carbon coating and the matrix is TiC, only the duplex coating with QC-TiC effectively inhibits the interfacial reaction, exhibiting significantly different behaviour as a protective barrier compared with the reaction compound TiC arising from C single coating and RC-TiC coating. In order to further elucidate the mechanism, the detailed microstructural features of the interfacial zones of as-prepared SiC<sub>f</sub>/C/QC-TiC/Ti17 composite were investigated by TEM, and compared to as-prepared SiC<sub>f</sub>/C/Ti17 composites. For as-prepared SiC<sub>f</sub>/C/Ti17 composites, interfacial zones have been identified to consist of different-sized TiC<sub>x</sub> layers, including a fine-grained TiC<sub>x</sub> layer with few amorphous C located at grain boundaries near the carbon coating, a transition-grained TiC<sub>x</sub> layer with non apparent amorphous C in the middle zone, and a coarse-grained TiC<sub>x</sub> layer adjacent to the Ti matrix. The grain size ranges from ~10 nm in the fine-grained TiC<sub>x</sub> layer to ~300nm in coarse-grained TiC<sub>x</sub> layer, resulting from continuous C diffusion from the C coating across the TiC layer, and gradual growth of matrix grains during consolidation [10,26]. As a result, there is also a C concentration gradient across the whole TiC<sub>x</sub> reaction zone, gradually declining from fine-grained TiC<sub>x</sub> layer to coarse-grained TiC<sub>x</sub> layer. This structure allows for short-circuit diffusion and intracrystalline diffusion due to the aggregation of amorphous carbon at grain boundaries in the fine-grained TiC<sub>x</sub> layer, and the high concentration of C vacancies in sub-stoichiometric TiC respectively. Furthermore, defects such as voids or microcracks may also be present in the TiC layer induced by the interfacial reaction [9] due to the change in volume. These three factors combined (short-circuit diffusion caused by intercrystalline amorphous C, intracrystalline diffusion due to sub-stoichiometric and defects induced by volume change) accelerate C diffusion at high temperatures of 1200°C. Therefore, the deleterious interfacial reaction at high temperatures rapidly exhausts the carbon coating leading to further damage of the SiC fibre.

Examining the C/RC-TiC duplex coating, the growth of small TiC grains is limited by amorphous carbon in the RC-TiC coating, as depicted in Fig. 2a and 2c. Consequently, carbon may rapidly diffuse through the RC-TiC layer via grain boundaries where amorphous carbon assembles, similar to the fine-grained TiC<sub>x</sub> layer in the C single coating, where short-circuit diffusion is still the dominant mechanism responsible for fast C diffusion at 1200 °C [27], causing the faster increase in the thickness of the entire TiC<sub>x</sub> layer than C/RC-TiC duplex coating.

In contrast to the C single coating which forms a TiC<sub>x</sub> interfacial reactive layer with a large gradient in C composition and grain size, TEM examination of the interfacial zone for the as-fabricated SiC<sub>f</sub>/C/QC-TiC/Ti17 composite (Fig. 4) shows much smaller gradients. Upon examination of the micrograph, a 0.8 μm reaction layer is apparent which corresponds to the original reactive sputtering deposited QC-TiC coating. The coating was originally deposited with a thickness of ~0.8 μm, thus no additional reactive TiC<sub>x</sub> layer formed, which suggests that the deposited QC-TiC effectively inhibits the deleterious interfacial reaction during HIP processing at 920°C, remaining almost inert in preventing C diffusion at this relative low temperature. Although the thickness of the deposited QC-TiC layer during composite HIP processing is unchanged, the grain structure of this layer coarsened from around 10 nm to several hundred nanometer, with a narrow 100 nm layer of ~ 50 nm grains adjacent to the amorphous carbon layer, and a wider ~700 nm thick layer of > 500 nm grains adjacent to the Ti matrix (shown in Fig. 4a and 4b). It's interesting that two layers of different grain size have emerged after HIPing the uniformly deposited TiC<sub>x</sub> coating at 920°C. Through closer observation on the fine-grained TiC<sub>x</sub> layer at higher magnification, a small amount of amorphous carbon is observed at TiC grain boundaries near the C coating, which was not present before HIP consolidation, as shown in Fig. 4c and 4d. It is evidence that the adjacent amorphous carbon can diffusion along TiC grain boundaries during TiC<sub>x</sub> grain growth during HIP consolidation, thus limiting TiC grain growth and forming the thin fine-grained TiC<sub>x</sub> layer observed, which can itself act as a short-circuit diffusion path. Accordingly, the observed superior diffusion inhibition of the C/QC-TiC duplex coating likely contributes to the formation of the coarse-grained TiC<sub>x</sub> layer.

Furthermore, the C concentration across the deposited TiC zone has been measured (as shown in Table 1, spot A1 to A5). A hyper-stoichiometric C concentration appears in the fine-grained  $\text{TiC}_x$  layer close to the carbon coating, while the coarse-grained  $\text{TiC}_x$  layer is quasi stoichiometric, unlike the steep C gradient in a C single coating. Thus, though there is a quite thin fine-grained  $\text{TiC}_x$  layer serving as short-circuit diffusion layer, the main constitution of deposited  $\text{TiC}_x$  layer after 920 °C HIPping is still coarse-grained, quasi stoichiometric  $\text{TiC}_x$ .

Considering the interfacial reaction mechanism, the interfacial reaction occurs when C diffuses into the Ti matrix and reacts with the  $\alpha\text{-Ti}/\beta\text{-Ti}$  phase [10,26], while there is hardly C diffusion through the existing QC-TiC layer due to obstruction by the quasi-stoichiometric coarse-grained  $\text{TiC}_x$  layer. As such, larger coarse grained ( $>500$  nm) quasi-stoichiometric  $\text{TiC}_x$  in the  $\text{SiC}_f/\text{C}/\text{QC-TiC}/\text{Ti17}$  composite should more effectively inhibit C diffusion than the coarse-grained ( $>100$  nm) sub-stoichiometric  $\text{TiC}_x$  in  $\text{SiC}_f/\text{C}/\text{Ti17}$  composite.

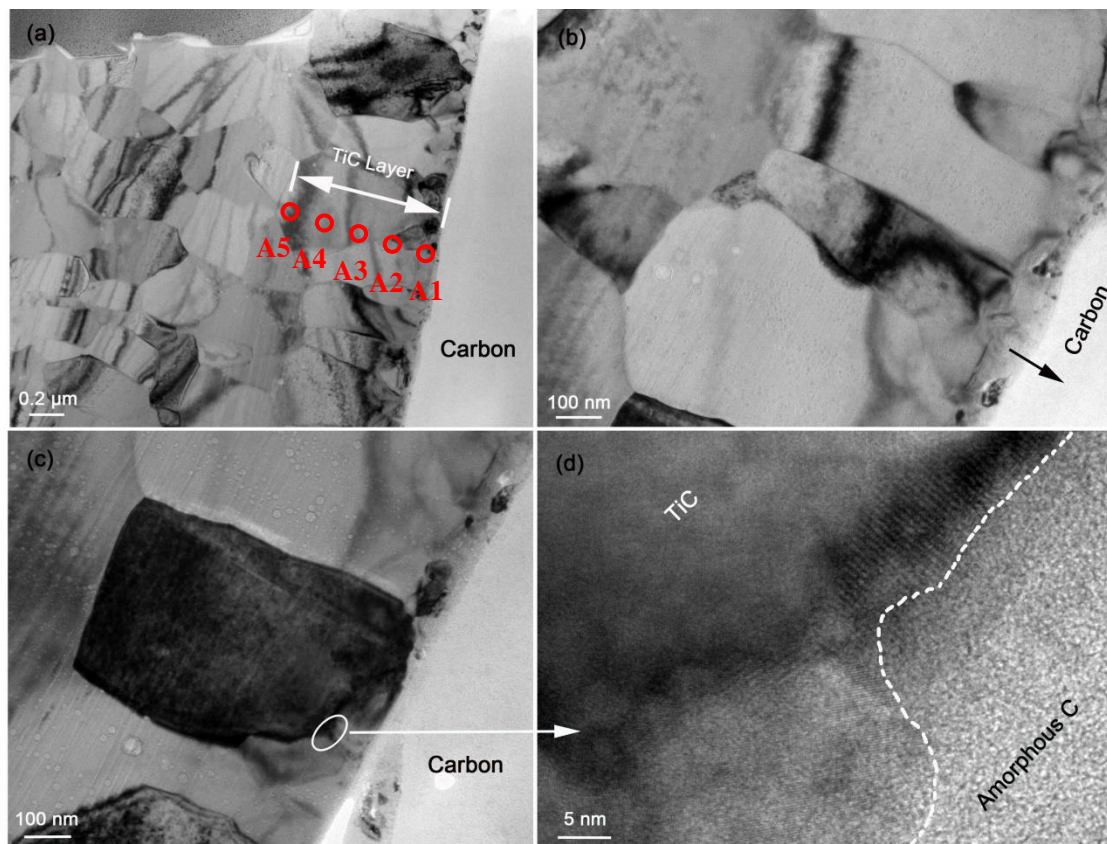


Fig. 4 TEM images of (a) interfacial zone for  $\text{C}/\text{TiC}_x$  and  $\text{TiC}_x/\text{Ti17}$  matrix and (b) interfacial zone for the as-fabricated  $\text{SiC}_f/\text{C}/\text{QC-TiC}/\text{Ti17}$  composite, high

magnification image for (c) interfacial zone nearby carbon coating and (d) boundary between two  $TiC_x$  grains in the TiC layer adjacent to the carbon coating.

Table 1 - C and Ti content as measured by EDS for five spots across the reaction layer (identified in fig. 4a) in a composite with C/QC-TiC duplex coating before and after 1200°C /1h heat exposure, respectively.

As processed			1200°C/1h exposed		
SiC <sub>f</sub> /C/ QC-TiC /Ti17 composite			SiC <sub>f</sub> /C/QC-TiC/Ti17 composite		
Sample No.	C (at.%)	Ti (at.%)	Sample No.	C(at.%)	Ti (at.%)
A1	55.6	40.9	B1	88.1	11.9
A2	47.5	48.5	B2	60.9	39.1
A3	46.6	49.8	B3	53.6	46.4
A4	46.3	50.8	B4	52.1	47.9
A5	46.5	51.2	B5	51.2	48.8

In order to inspect the interfacial evolution for SiC<sub>f</sub>/C/QC-TiC/Ti17 composite, the TEM sample for SiC<sub>f</sub>/C/QC-TiC/Ti17 composite after 1200 °C exposure was investigated. As Fig. 5a and 5b shown, in contrast to as-deposited SiC<sub>f</sub>/C/QC-TiC/Ti17 composite, the  $TiC_x$  grains in close proximity to the carbon coating have grown and coarsened from the original ~50 nm to 200~300 nm after heat treatment, which can be understood as the original fine-grained  $TiC_x$  layer having disappeared and a new ~400 nm thick transition-grained  $TiC_x$  layer formed. This is analogous to the microstructural evolution of a C single coating system after heat treatment at 1100°C for 2 hr [10]. Moreover, the coarse-grained  $TiC_x$  layer thickened to  $> 4 \mu m$  from the initial ~700 nm thick as prepared layer. It's worthy noticing that the thickness of the coarse-grained  $TiC_x$  layer ( $> 4 \mu m$ ) far exceeds the thickness of transition-grained  $TiC_x$  layer (~ 400 nm), which may be evidence that the thickening of transition-grained  $TiC_x$  layer is confined during high temperature exposure. In addition, the EDS results for spot B1 to B5 along the  $TiC_x$  layer growth direction indicated that carbon content is fairly high in the transition  $TiC_x$  layer, and gradually decreases to quasi-stoichiometric in the coarse-

grained  $TiC_x$  layer (see Table 1). Compared with the as-fabricated  $SiC_{\beta}/C/QC-TiC/Ti17$  composite, the thickening of the hyperstoichiometric reaction layer after 1200 °C exposure probably originates from more carbon direct diffusion into the TiC grains boundaries. As evidenced in Fig. 5c and 5d, significant amounts of amorphous carbon are observed between two grains in the transition-grained  $TiC_x$  layer adjacent to the inner C coating, accounting for the increased carbon content in this area and restricted grain growth in the transition-grained  $TiC_x$  layer. Fortunately, the thick, coarse-grained  $TiC_x$  layer still maintains quasi-stoichiometry which effectively hinders C diffusion at high temperature due to its dense, (relatively) vacancy free crystalline structure [28]. Thus, the deposited quasi-stoichiometric  $TiC_x$  coating can evolve into coarsened grains with uniform composition and grain size during HIP consolidation, which provide better protection for SiC fibres and achieve better interface stability for the  $SiC_{\beta}/Ti17$  composite even at 1200°C relative to C single coating and C/RC-TiC duplex coating. This is due to low intracrystalline C diffusion through the thick, quasi-stoichiometric  $TiC_x$  layer.

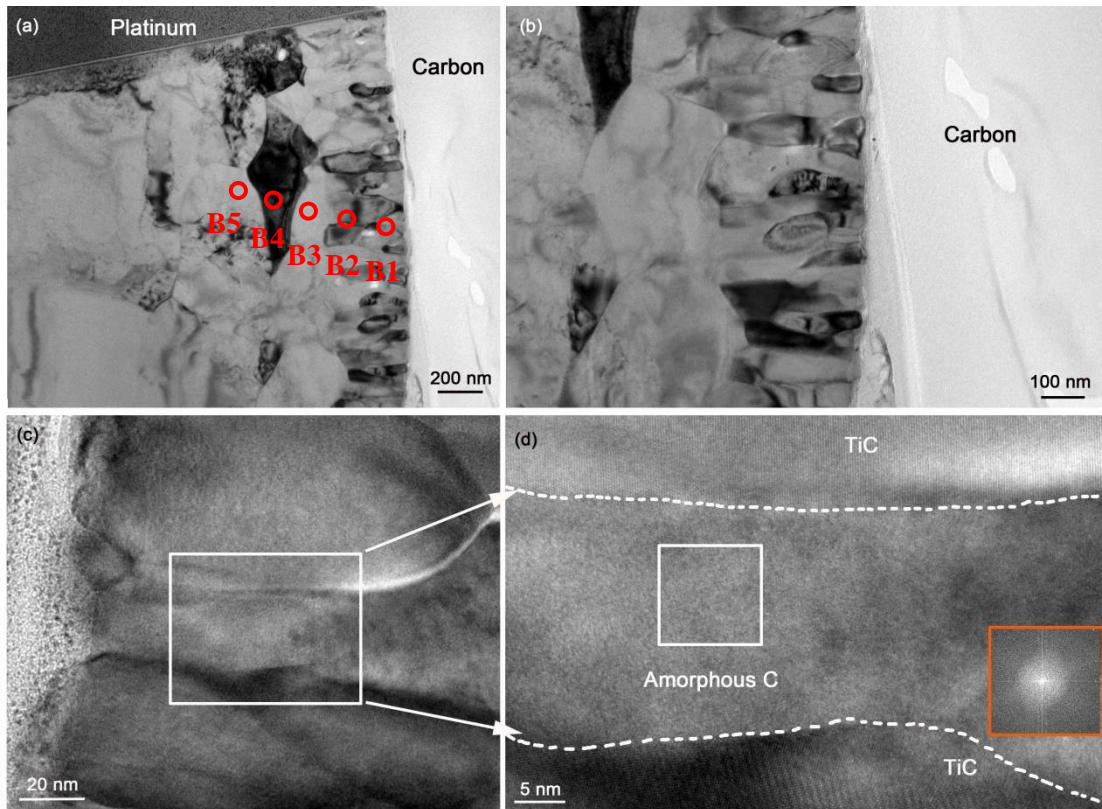


Fig. 5 TEM images of : (a) interfacial zone and matrix and (b) interfacial zone for



1200°C/1h exposed SiC<sub>f</sub>/C/QC-TiC/Ti17 composite, high magnification image for (c) interfacial zone nearby carbon coating and (d) the magnification image for the area in the white square frame of (c), the inset chart of orange square frame is the diffraction pattern for the white square frame area.

#### **4. Conclusions**

In conclusion, the deposited carbon/ QC-TiC duplex coating offers a significant improvement in the chemical stability of SiC<sub>f</sub>/Ti-alloy composites at high temperature relative to C single coatings and C/RC-TiC duplex coatings. Specifically, the interfacial reaction layer has structural and compositional gradients in the single layer carbon coating, leading to short-circuit diffusion due to the presence of amorphous carbon concentrating at grain boundary of a fine-grained TiC layer, and intracrystalline based diffusion supplied by C vacancies existing in a coarse-grained sub-stoichiometric TiC layer. This results in failure of SiC fibre protection at 1200 °C. In addition, in the C/ RC-TiC duplex coating, TiC nanograins are surrounded by amorphous carbon that also served as short-circuit diffusion paths, giving rise to a similar failure mechanism as the simple carbon coating at high temperatures. In contrast, the introduction of a C/QC-TiC duplex coating can effectively prevent carbon diffusion induced by amorphous carbon-caused short-circuit diffusion and sub- stoichiometric-caused intracrystalline diffusion in the simple carbon coating. This is achieved by the formation of a compact, quasi-stoichiometric coarse-grained TiC layer. Thus, C/QC-TiC duplex coatings can provide much better protection for SiC fibres even at high temperatures of 1200°C by comparison to C single coatings and C/RC-TiC duplex coatings, which open new avenues for high-temperature reaction barrier coatings for SiC<sub>f</sub>/Ti composites.

#### **Acknowledgements**

The authors thank the Natural Science Foundation of China for financial support, grant no. 51571128. The authors also wish to thank M. L. Jackson for his useful comments and feedback.

#### **References**

1. Osborne D, Ghonem H. Experimental and computational study of interphase properties and mechanics in titanium metal matrix composites at elevated temperatures. USAF office of scientific research bolling air force base,2005;DC 20332: 47.
2. Phillip J Doorbar, Stephen Kyle-Henney. Development of continuously-reinforced metal matrix composites for aerospace applications, 2018.
3. S.Haque, K.L.Choy. Finite element modelling of the effect of a functionally graded protective coating for SiC monofilaments on Ti-based composite behavior. Mater. Sci. Eng. A. 2000;291:97-109.
4. H. Izui, S. Kinbara and M. Okano, Pulse Electric Current Synthesis and Processing of Materials, 2006, 289.
5. A. Muthuchamy, G.D. Jannaki Ram, V. Subramanya Sarma. Spark plasma consolidation of continuous fibre reinforced titanium matrix composites. Mater. Sci. Eng. A. 2017;703:461-469.
6. I.W.Hall, J.L.Lirn, J.Rizza. Interfacial reactions in titanium matrix composites. Journal of materials science letters.1991;10:263-366.
7. Y.W.Xun, M.J.Tan, J.T.Zhou. Processing and interface stability of SiC fibre reinforced Ti-15V-3Cr matrix composites. J. mater. Process. tech. 2000;102:215-220.
8. Y.C. Fu, N.L. Shi, D.Z. Zhang, R. Yang. Effect of C coating on the interfacial microstructure and properties of SiC fibre-reinforced Ti matrix composites. Mat. Sci. Eng.2006; A 426: 278.
9. Z.X. Guo and B. Derby. Solid state fabrication and interfaces of fibre reinforced metal matrix composites. Prog. Mater. Sci.1995; 39:411-495.
10. M. Wu, K. Zhang, and M. Wen. Temperature-dependent evolution of interfacial zones in SiC<sub>f</sub>/C/Ti17 composites. RSC Advances.2017;7(72):45327-45334.
11. Choy, K. L. and Derby, B., The compatibility of TiB<sub>2</sub> protective coatings with SiC fibre and Ti-6Al-4V, Journal of Microscopy,1993;169(2): 289.
12. Z. Fan, Z.X. Guo and B. Cantor. The kinetics and mechanism of interfacial reaction in sigma fibre-reinforced TiMMCs. Compos. Part A. 1997;28A:131-140.



13. F.C. Ma, S.Y. Lu, and P. Liu. Microstructure and mechanical properties variation of TiB/Ti matrix composite by thermos-mechanical processing in beta phase field, *J. Alloy. Compd.* 2017;695:1515-1522.
14. W. Zhang, Y.Q. Yang, and G.M. Zhao, etc. Interfacial reaction studies of B<sub>4</sub>C-coated and C-coated SiC fibre reinforced Ti-43Al-9V composites. *Intermetallics*, 2014;50:14-19.
15. S.M. Jeng. W. Kai, and C.J. Shih. Interface reaction studies of B<sub>4</sub>C/B and SiC/B fibre-reinforced Ti<sub>3</sub>Al matrix composites. *Mat. Sci. Eng. A.* 1989;114:189-196.
16. X. Luo, X. Ji, and Y.Q. Yang. Microstructure evolution of C/Mo double-coated SiC fibre reinforced Ti<sub>6</sub>Al<sub>4</sub>V composites. *Mat. Sci. Eng. A.* 2014;597,95-101.
17. W. Sai, H.Z. Zhao, and F. C. Wang. Effect of Ti content and sintering temperature on the microstructures and mechanical properties of TiB reinforced titanium composites synthesized by SPS process. *Mat. Sci. Eng. A.* 2013;560:249-255.
18. X.W. Tao, Z.J. Yao, etc. Investigation on microstructure, mechanical and tribological properties of in-situ (TiB+TiC)/Ti composite during the electron beam surface melting, *Surf. Coat. Technol.*, 337 (2018) 418-425.
19. Choy, K. L. and Derby, B., The evaluation of the efficiency of TiB<sub>2</sub> and TiC as protective coatings for SiC monofilament in Ti-based composites, *Journal of Materials Science*, 1994; 29(4) 3774.
20. K. Vasanthakumar and Srinivasa Rao Bakashi. Effect of C/Ti ratio on densification, microstructure and mechanical properties of TiC<sub>x</sub> prepared by reactive spark plasma sintering. *Ceramics International*. 2018;44:484-494.
21. Y.D. Su, X.M. Wang, and H.M. Wang. Grain-size effect on the preferred orientation of TiC/ $\alpha$ -C:H thin films. *Appl. Surf. Sci.* 2012;258:6800-6806.
22. Nikolett Olah, Zsolt Forgarassy, Attila Sulyok. TiC crystallite formation and the role of interfacial energies on the composition during the deposition process of TiC/ $\alpha$ :C thin films. *Surf. Coat. Technol.* 2016;302:410-419.
23. D.Q. He, L.L. Shang, etc. Tailoring the mechanical and tribological properties of B<sub>4</sub>C/ $\alpha$ -C coatings by controlling the boron carbide content. *Surf. Coat. Technol.*, 329(2017) 11-18.

24. M. Wu, K. Zhang, and M. Wen. Interfacial reactions in SiC<sub>f</sub>/C/Ti17 composites dominated by texture of carbon coatings. *Carbon*. 2017;124:238-249.
25. K. Nygren, M. Smuelsson, and H. Arwin. Optical methods to quantify amorphous carbon in carbide-based nanocomposite coatings. *Thin solid films*. 2017;638:291-297.
26. M.J. Wang, H. Huang, etc. Microstructure and interfacial strength of SiC fibre reinforced Ti17 alloy composites with different consolidation temperatures. *Rare Metals*.2018.
27. S.Q. Guo, Y. Kagawa, H. Saito, C. Masuda. Microstructural characterization of interface in SiC fibre-reinforced Ti-15V-3Cr-3Al-3Sn matrix composite. *Mater. Sci. Eng. A*.1998; 246: 25.
28. X. X. Yu, Gregory B. Thompson, and Christopher R. Weinberger. Influence of carbon vacancy formation on the elastic constants and hardening mechanism in transition metal carbides. *J. Eur. Ceram. Soc.*, 2015;35:95-103.